

Directly Observed Halocarbene–Halocarbanion Equilibration

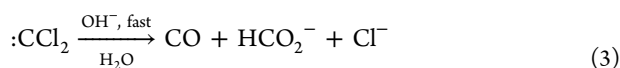
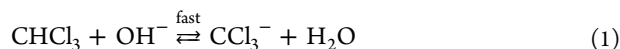
Lei Wang, Robert A. Moss,* and Karsten Krogh-Jespersen

Department of Chemistry & Chemical Biology, Rutgers, The State University of New Jersey, New Brunswick, New Jersey 08903, United States

S Supporting Information

ABSTRACT: Equilibria between phenylhalocarbenes, halide ions, and phenyldihalomethide carbanions have been spectroscopically characterized and computationally investigated for the halogens Cl and Br. Equilibrium constants, forward and reverse rate constants, and associated thermodynamic parameters are reported.

Hine's classic mechanism for the hydrolysis of chloroform, summarized in eqs 1–3, features a rate-determining dissociation of the trichloromethide carbanion to give dichlorocarbene and chloride (eq 2).¹ Hine later found that bromide and iodide could trap CCl_2 to form the CCl_2Br^- and CCl_2I^- carbanions, respectively,² indicating that eq 2 is very likely reversible, one of a family of dihalocarbene–trihalomethide equilibria.



We demonstrated the reverse of eq 2 spectroscopically: laser flash photolysis (LFP) of dichlorodiazirine in the presence of tetrabutylammonium chloride (TBACl) produced CCl_2 ,³ which was captured by chloride to give CCl_3^- , visible at 328 nm.⁴ Similarly, CCl_2 was captured by bromide to yield CCl_2Br^- , absorbing at 388 nm.⁴ Unfortunately, the weak absorbance of CCl_2 precluded a direct LFP study of $\text{CCl}_2/\text{CCl}_3^-$ equilibration.^{5,6}

In contrast, phenylhalocarbenes absorb strongly⁷ and should be well-suited to a study of the equilibria described in eq 4, where $X = \text{Cl}$ or Br . Indeed, manipulation of these equilibria by variation of the halide ion concentration enables additions of electrophilic PhCX or nucleophilic PhCX_2^- to electron-rich or electron-poor alkenes, respectively.^{8,9} LFP measurements of the rate constants for the competitive additions of PhCBr and PhCBr_2^- to tetramethylethylene or acrylonitrile, together with the rate constant for addition of Br^- to PhCBr as a function of bromide ion concentration, permitted an estimate of $K = 2.8 \text{ M}^{-1}$ for the equilibrium of eq 4 with $X = \text{Br}$.⁸ It should be noted, however, that the latter value was determined in acetonitrile/tetrahydrofuran and might be solvent-dependent.



Here we are pleased to describe the *first directly observed* halocarbene–halocarbanion equilibria, including values of the equilibrium constants, forward and reverse rate constants, and associated thermodynamic parameters.

LFP of phenylchlorodiazirine¹⁰ in 1,2-dichloroethane (DCE) at 351 nm gives PhCCl , whose UV–vis spectrum after calibration¹¹ features a strong $\pi \rightarrow \text{p}$ absorption at 292 nm and a weak $\sigma \rightarrow \text{p}$ absorption at 604 nm⁷ (see Figure 1). The

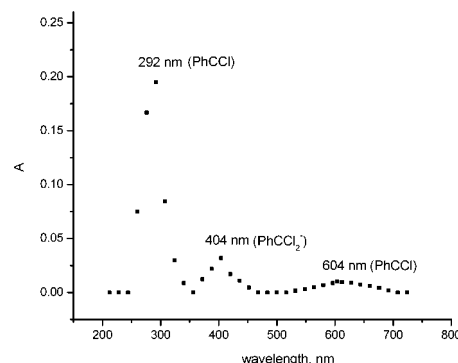


Figure 1. UV–vis spectrum acquired 88 ns after LFP of phenylchlorodiazirine with 0.61 M TBACl in DCE (after calibration). Absorptions of PhCCl are at 292 and 604 nm; the absorption of PhCCl_2^- is at 404 nm.

PhCCl absorptions were computed to have $\lambda = 292 \text{ nm}$ [oscillator strength (f) = 0.4740] and 705 nm ($f = 0.0025$).¹² In the presence of TBACl, a new absorption due to PhCCl_2^- appears at 404 nm (computed¹² $\lambda = 390 \text{ nm}$, $f = 0.1999$). PhCCl_2^- also contributes to the absorption peak at 292 nm, but in a minor fashion (a transition was computed with $\lambda = 297 \text{ nm}$ and $f = 0.0749$).¹²

In accord with eq 4 ($X = \text{Cl}$), the ratio of the PhCCl absorbance at 292 nm to the PhCCl_2^- absorbance at 404 nm varies with $[\text{TBACl}]$: A_{292}/A_{404} decreases with increasing TBACl, and as expected for an equilibrium, the ratio remains relatively constant from 120 to 250 ns after the laser flash [see Figure S-2 in the Supporting Information (SI)]. An average value of A_{292}/A_{404} was determined over the 150–200 ns time interval at TBACl concentrations of 0.105, 0.150, 0.186, 0.346, and 0.611 M (see Figure S-2). Data analysis employed the Beer–Lambert law, using computed oscillator strengths in place of the unknown extinction coefficients of PhCCl and PhCCl_2^- ;^{13,14} details appear in the SI. Thus, a plot of $A_{292}/$

Received: September 4, 2012

Published: October 11, 2012

A_{404} versus $1/[\text{TBACl}]$ afforded the linear correlation shown in Figure 2, whose slope (0.591) leads to $K = 4.01 \text{ M}^{-1}$ for eq 4

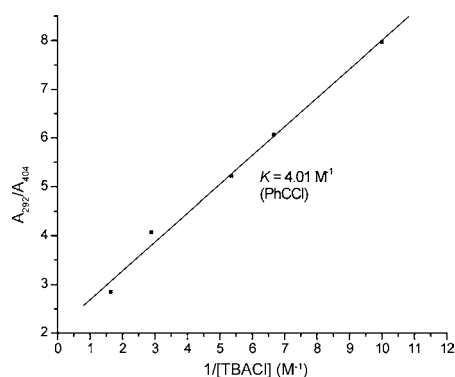


Figure 2. Calibrated absorption intensities of PhCCl at 292 nm relative to PhCCl₂⁻ at 404 nm vs $1/[\text{TBACl}]$ in DCE at 294 K. The slope of the correlation line is 0.591 ($r = 0.996$), leading to $K = 4.01 \text{ M}^{-1}$ for eq 4 ($X = \text{Cl}$).

($X = \text{Cl}$) at 294 K.¹⁵ We caution that this value could be specific to the DCE solvent and ignores possible solvent-dependent aggregation of the TBACl.

We determined K at four additional temperatures (262, 273.4, 284, and 309.6 K; see Figures S-7–S-10) and obtained K values of 12.3, 7.34, 5.12, and 2.61 M^{-1} , respectively. The correlation of $\ln K$ versus $1/T$ is shown in Figure 3, and its slope and intercept afford $\Delta H^\circ = -5.7 \pm 0.3 \text{ kcal/mol}$, $\Delta S^\circ = -16.8 \pm 1.1 \text{ eu}$, and $\Delta G^\circ(298 \text{ K}) = -0.71 \text{ kcal/mol}$.

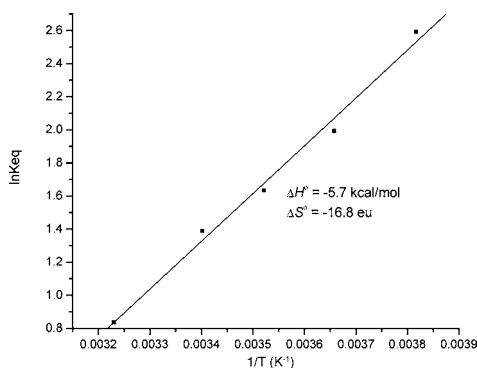


Figure 3. Plot of $\ln K$ vs $1/T$ for the equilibrium in eq 4 ($X = \text{Cl}$). The slope (2887.3 K) affords $\Delta H^\circ = -5.7 \pm 0.3 \text{ kcal/mol}$, and the intercept (-8.49) gives $\Delta S^\circ = -16.8 \pm 1.1 \text{ eu}$. The correlation coefficient was $r = 0.996$.

In a completely parallel manner, we determined the equilibrium constants and thermodynamic parameters for eq 4 with $X = \text{Br}$. LFP of phenylbromodiazirine^{10a} in DCE afforded PhCBr,⁷ whose calibrated¹¹ UV-vis spectrum (Figure 4) displayed $\pi \rightarrow p$ and $\sigma \rightarrow p$ absorptions at 316 and 620 nm, respectively (computed values:¹² $\lambda = 311 \text{ nm}$, $f = 0.4326$ and $\lambda = 747 \text{ nm}$, $f = 0.0017$). Addition of TBABr produced PhCBr₂⁻, which generated a new absorption peak at 428 nm (computed $\lambda = 463 \text{ nm}$, $f = 0.1370$;¹² an additional absorption from PhCBr₂⁻ with $\lambda = 320 \text{ nm}$, $f = 0.0904$ was also computed).

The A_{316}/A_{428} ratio remained relatively constant from 200 to 300 ns after the laser flash (see Figure S-12). An average value of A_{316}/A_{428} was determined over the 200–250 ns time interval at TBABr concentrations of 0.100, 0.150, 0.197, 0.394, and

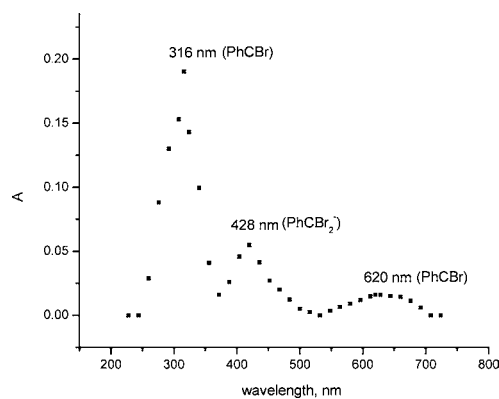


Figure 4. UV-vis spectrum acquired 80 ns after LFP of phenylbromodiazirine with 0.10 M TBABr in DCE (after calibration). Absorptions of PhCBr are at 316 and 620 nm; the absorption of PhCBr₂⁻ is at 428 nm.

0.797 M (see Figure S-12). Analysis as for the PhCCl data (see above) gave a linear correlation for A_{316}/A_{428} versus $1/[\text{TBABr}]$ (Figure S-17), whose slope (1.049) afforded $K = 3.01 \text{ M}^{-1}$ at 294 K.¹⁵ This directly measured value of K for eq 4 ($X = \text{Br}$) is in excellent agreement with our previously extracted indirect value of 2.8 M^{-1} ,⁸ despite differences in the solvent.

K was measured at four additional temperatures (259.7, 270.6, 283.7, and 308.1 K; see Figures S-18–S-21), leading to K values of 4.68, 3.98, 3.46, and 2.60 M^{-1} , respectively. The correlation of $\ln K$ versus $1/T$ is shown in Figure S-22, and its slope and intercept afford $\Delta H^\circ = -1.91 \pm 0.05 \text{ kcal/mol}$, $\Delta S^\circ = -4.32 \pm 0.16 \text{ eu}$, and $\Delta G^\circ(298 \text{ K}) = -0.62 \text{ kcal/mol}$.

With these values of K for eq 4 and the fact that $K = k_1/k_{-1}$, we can obtain the reverse rate constant k_{-1} by determining the forward rate constant, k_1 . Accordingly, we measured k_1 for the reaction of PhCCl with Cl⁻ in DCE using LFP by following the appearance of PhCCl₂⁻ at 404 nm as a function of $[\text{TBACl}]$. The resulting correlation is shown in Figure S-23, and its slope yields $k_1 = 1.97 \times 10^8 \text{ M}^{-1} \text{ s}^{-1}$. Given that $K = 4.01 \text{ M}^{-1}$ for eq 4 ($X = \text{Cl}$) at 294 K, $k_{-1} = 4.91 \times 10^7 \text{ s}^{-1}$.

Similarly, we determined k_1 for the quenching of PhCBr by Br⁻ in DCE. The correlation of k_{app} for the formation of PhCBr₂⁻ at 428 nm versus $[\text{TBABr}]$ in DCE is shown in Figure S-24, and its slope affords $k_1 = 3.55 \times 10^7 \text{ M}^{-1} \text{ s}^{-1}$. Given that $K = 3.01 \text{ M}^{-1}$ for eq 4 ($X = \text{Br}$) at 294 K, $k_{-1} = 1.18 \times 10^7 \text{ s}^{-1}$.

Experimental data for the equilibria of eq 4 are collected in Table 1. The formation of PhCX₂⁻ from PhCX and X⁻ is very rapid when $X = \text{Cl}$ or Br, but the dissociation of the carbanion is similarly fast, so K is only 3–4 M⁻¹. The enthalpy of carbanion formation is clearly favorable, but it is opposed by the unfavorable entropy associated with the conversion of two reactants into a single product, so ΔG° is only slightly negative. The computed values of the thermodynamic parameters for eq 4 (see Table S-1 in the SI) are more negative than the experimental values in Table 1. For example, at the M06-2X/6-311+G(d) level, $\Delta H^\circ_{\text{comp}} = -10.4$ (Cl) or -8.4 (Br) kcal/mol, and $\Delta G^\circ_{\text{comp}} = -3.7$ (Cl) or -2.0 (Br) kcal/mol, while the $\Delta S^\circ_{\text{comp}}$ values are approximately -20 eu . At the CCSD(T)/6-311+G(d) level, we obtained $\Delta H^\circ_{\text{comp}}$ values of -10.1 (Cl) and -7.1 (Br) kcal/mol. The halocarbanion formation reaction (eq 4) is thus $\sim 3 \text{ kcal/mol}$ more exothermic, both experimentally and computationally, when $X = \text{Cl}$ relative to $X = \text{Br}$. Presumably, the increase in reaction favorability partly reflects the larger C–X bond strength anticipated for $X = \text{Cl}$.

Table 1. Experimental Data for the Equilibria of Equation 4

carbene	K (M^{-1})	k_1 ($M^{-1} s^{-1}$)	k_{-1} (s^{-1})	ΔH° (kcal/mol)	ΔS° (eu)	ΔG° (kcal/mol)
PhCCl	4.01	19.7×10^7	4.91×10^7	-5.7	-17	-0.71 ^a
PhCBr	3.01	3.55×10^7	1.18×10^7	-1.9	-4.3	-0.62 ^a

^aAt 298 K; the probable uncertainties in ΔG° are ± 0.06 (PhCCl) and ± 0.03 (PhCBr) (kcal/mol).

The numerical disparities between the computed and experimental thermodynamic values may in part result from an inadequate representation of the experimental solution in the computational studies. For example, the calculations did not consider the dissolved ions explicitly or even implicitly (e.g., via the applied continuum solvation model; see the SI). Halide and halocarbanion interactions with the TBA cations, in particular, are likely to affect the measured thermodynamic parameters significantly.

For the addition of Cl^- to CCl_2 (the reverse of eq 2 above), we found $\Delta H_{comp}^\circ = -15.4$ kcal/mol, $\Delta S_{comp}^\circ = -19$ eu, and $\Delta G_{comp}^\circ = -9.8$ kcal/mol at the M06-2X/6-311+G(d) level. At the CCSD(T)/6-311+G(d) level, we obtained $\Delta H_{comp}^\circ = -12.1$ kcal/mol. The increase in reaction exothermicity computed for the addition of Cl^- to CCl_2 relative to PhCCl suggests that the energetic stabilization afforded through the σ -inductive effect by a Cl atom bonded to the carbanionic center is larger than the π -resonance stabilization provided by an analogously bonded phenyl group.

In conclusion, the experimentally determined equilibrium constants for eq 4 ($X = Cl, Br$) are 3–4 M^{-1} , and the ΔG° values are -0.6 to -0.7 kcal/mol. From the synthetic chemist's viewpoint, K values near unity imply that either electrophilic PhCX or nucleophilic PhCX₂⁻ can be made available as desired simply by adjusting the halide ion concentration. This provides a simple but effective “umpolung” of normally electrophilic carbenes.⁸

■ ASSOCIATED CONTENT

📄 Supporting Information

Spectroscopic data, methodology for determination of K , and computational details and results. This material is available free of charge via the Internet at <http://pubs.acs.org>.

■ AUTHOR INFORMATION

Corresponding Author

moss@rutchem.rutgers.edu

Notes

The authors declare no competing financial interest.

■ ACKNOWLEDGMENTS

We are grateful to the National Science Foundation for financial support.

■ REFERENCES

- (1) Hine, J. *J. Am. Chem. Soc.* **1950**, *72*, 2438.
- (2) Hine, J.; Dowell, A. M., Jr. *J. Am. Chem. Soc.* **1954**, *76*, 2688.
- (3) Moss, R. A.; Tian, J.; Sauers, R. R.; Ess, D. H.; Houk, K. N.; Krogh-Jespersen, K. *J. Am. Chem. Soc.* **2007**, *129*, 5167.
- (4) Moss, R. A.; Zhang, M.; Krogh-Jespersen, K. *Org. Lett.* **2009**, *11*, 5702.
- (5) Chu, G.; Moss, R. A.; Sauers, R. R. *J. Am. Chem. Soc.* **2005**, *127*, 14206.
- (6) CCl_2 has been observed at 440–560 nm in a cryogenic matrix. See: Milligan, D. E.; Jacox, M. E. *J. Chem. Phys.* **1967**, *47*, 703.

(7) The strong absorbance of PhCCl at ~ 300 nm is due to a π (phenyl) to p(carbene) charge-transfer transition, which is absent in CCl_2 . See: Pliego, J. R.; De Almeida, W. B.; Celebi, S.; Zhu, Z.; Platz, M. S. *J. Phys. Chem. A* **1999**, *103*, 7481. Also see: Gould, I. R.; Turro, N. J.; Butcher, J., Jr.; Doubleday, C., Jr.; Hacker, N. P.; Lehr, G. F.; Moss, R. A.; Cox, D. P.; Guo, W.; Munjal, R. C.; Perez, L. A.; Fedorynski, M. *Tetrahedron* **1985**, *41*, 1587.

(8) Moss, R. A.; Tian, J. *J. Am. Chem. Soc.* **2005**, *127*, 8960.

(9) For an independent computational study of these competitive reactions, see: Fang, R.; Ke, Z.; Shen, Y.; Zhao, C.; Phillips, D. L. *J. Org. Chem.* **2007**, *72*, 5139.

(10) (a) Graham, W. H. *J. Am. Chem. Soc.* **1965**, *87*, 4396. (b) The diazine exhibits maxima at 369, 384, and 389 nm in pentane. It was used with $A_{369} \approx 0.5$.

(11) Calibration was used to correct the intensities of the initial UV–vis absorptions for wavelength-dependent variations in sample absorptivity, xenon monitoring lamp emission, and detector sensitivity from 244 to 804 nm. The calibration curves are shown in Figures S-1 and S-11 in the SI.

(12) Electronic transitions were computed at the TD-B3LYP/6-311+G(d)//M06-2X/6-311+G(d) level. The CPCM solvent continuum dielectric model, simulating DCE, was applied in all of the calculations. See the SI for computational details and additional results.

(13) Moss, R. A.; Wang, L.; Odorisio, C. M.; Krogh-Jespersen, K. *J. Am. Chem. Soc.* **2010**, *132*, 10677.

(14) Formally, the computed oscillator strengths are proportional to the frequency-integrated absorption coefficients. Although the widths of the carbene and carbanion absorption bands differed, we did not attempt to correct for this. We conservatively estimated that the ratio $f_{carbene}/f_{carbanion}$ accurately reproduces the desired $\epsilon_{carbene}/\epsilon_{carbanion}$ ratio to within a factor of 2.

(15) $K = (\text{slope})^{-1}(f_2/f_1)$, where f_2 is the computed oscillator strength of PhCX and f_1 is the computed oscillator strength of PhCX₂⁻. For $X = Cl$, $f_2 = 0.4740$ for PhCCl at 292 nm and $f_1 = 0.1999$ for PhCCl₂⁻ at 390 nm (the computed maximum). For $X = Br$, $f_2 = 0.4326$ for PhCBr and $f_1 = 0.1370$ for PhCBr₂⁻.¹²